

Spectroscopic Studies of Phenyl Iron(IV) Porphyrin Complexes and Their Conversion into Iron(II) *N*-Phenylporphyrins

Alan L. Balch* and Mark W. Renner

Contribution from the Department of Chemistry, University of California, Davis, California 95616. Received September 3, 1985

Abstract: Oxidation of phenyl iron(III) tetraarylporphyrin complexes with bromine in chloroform at $-60\text{ }^{\circ}\text{C}$ produces deep-red solutions whose ^1H and ^2H NMR spectra indicate that they are the corresponding iron(IV) complexes. Characteristic ^1H NMR resonances include pyrrole protons at -60 to -70 ppm, iron phenyl resonances at ca. -300 ppm for the ortho protons, -50 to -75 ppm for the meta protons, ca. -100 ppm for the para protons, and ca. $+110$ ppm for the para-methyl protons. The magnetic susceptibility of the iron(IV) species is $2.6 \pm 0.4 \mu_{\text{B}}$. These aryl iron(IV) complexes are thermally unstable. When warmed, the aryl iron(IV) complex undergoes a clean reductive elimination to form the iron(II) complex of the *N*-arylporphyrin. The electronic structure of the $S = 1$ iron(IV) complexes is consistent with an orbital occupancy $d_{xy}^2 d_{xz}^1 d_{yz}^1$ with π -spin density transferred to the porphyrin and the axial phenyl group.

The chemical characterization of the σ -bonded phenyl iron(III) porphyrin complexes **1** have received considerable attention. These low-spin complexes have been isolated from the reaction of phenylmagnesium bromide or phenyllithium with haloiron(III) porphyrins¹⁻⁵ and have been subject to extensive characterization including both ^1H NMR spectroscopy⁴ and X-ray crystallography.⁶

The destruction of hemoglobin and myoglobin by arylhydrazines in the presence of dioxygen leads to the precipitation of Heinz bodies and the formation of green pigments which have been identified as *N*-phenylheme.⁷⁻⁹ Phenyl iron(III) porphyrins have been demonstrated as intermediates in this process by both ^1H NMR spectroscopy^{10,11} and by isolation, crystallization, and X-ray crystallography of phenylmyoglobin.¹² Studies on models have demonstrated that the transfer of the phenyl group from iron to nitrogen occurs under oxidizing conditions.¹³⁻¹⁵ Electrochemical and optical spectroscopic studies have suggested that this process occurs via several intermediates as shown in Scheme I.

This article is concerned with the first two steps in this scheme. Previous work involving spectroscopic studies of the iron(II) and iron(III) complexes of the *N*-substituted porphyrins has appeared.^{16,17} Here we are particularly concerned with the direct

observation of the iron(IV) complex **2**. Iron(IV) complexes generally are rare. One-electron oxidation of iron(III) porphyrin halide complexes generally yields products which are now acknowledged to be iron(III) complexes of oxidized porphyrin radicals.¹⁸⁻²⁶ Recently, however, the presence of the $(\text{Fe}^{\text{IV}}\text{O})^{2+}$ unit in the enzymatic intermediates, horseradish peroxidase compounds I and II, has become established through comparative studies on the actual enzyme intermediates and on synthetically prepared model compounds.²⁷⁻³⁵ The oxo ligand is particularly significant in stabilizing the high formal iron oxidation state, and the available evidence on the electronic structure, both from experiment²⁷⁻³⁵ and theory,^{36,37} indicates that the unpaired electrons in these $S = 1$ species are localized on the $\text{Fe}=\text{O}$ unit. The electronic distribution is altered when that oxo function is not present. Thus, $(\text{CH}_3\text{O})_2\text{FeTMP}$ (TMP is the dianion of tetramethylporphyrin), while still possessing an $S = 1$ ground state, displays different spectroscopic properties that indicate an altered electronic distribution within the complex.³⁸

- (1) Clarke, D. A.; Grigg, R.; Johnson, A. W. *J. Chem. Soc., Chem. Commun.* **1966**, 208.
- (2) Clarke, D. A.; Dolphin, D.; Grigg, R.; Johnson, A. W.; Plinck, H. A. *J. Chem. Soc. C* **1968**, 881.
- (3) Ogoshi, H.; Sugimoto, H.; Yoshida, Z.-I.; Kobayashi, H.; Sakai, H.; Maeda, Y. *J. Organomet. Chem.* **1982**, *234*, 185.
- (4) Cocolios, P.; Laviron, E.; Gullard, R. *J. Organomet. Chem.* **1982**, *228*, C39.
- (5) Cocolios, P.; Lagrange, G.; Gullard, R. *J. Organomet. Chem.* **1983**, *253*, 65.
- (6) Doppelt, P. *Inorg. Chem.* **1984**, *23*, 4009.
- (7) Saito, S.; Hano, H. A. *Proc. Natl. Acad. Sci. U.S.A.* **1981**, *78*, 5508.
- (8) Ortiz de Montellano, P. R.; Kunze, K. L. *J. Am. Chem. Soc.* **1981**, *103*, 6534.
- (9) Augusto, O.; Kunze, K. L.; Ortiz de Montellano, P. R. *J. Biol. Chem.* **1982**, *257*, 6231.
- (10) Kunze, K. L.; Ortiz de Montellano, P. R. *J. Am. Chem. Soc.* **1983**, *105*, 1380.
- (11) Ortiz de Montellano, P. R.; Kerr, D. E. *Biochemistry* **1985**, *24*, 1147.
- (12) Ringe, D.; Petsko, G. A.; Kerr, D. E.; Ortiz de Montellano, P. R. *Biochemistry* **1984**, *23*, 2-4.
- (13) Ortiz de Montellano, P. R.; Kunze, K. L.; Augusto, O. *J. Am. Chem. Soc.* **1982**, *104*, 3545.
- (14) Mansuy, D.; Battioni, J.-P.; Duprè, D.; Sartori, E.; Chottard, G. *J. Am. Chem. Soc.* **1982**, *104*, 6159.
- (15) Lancon, D.; Cocolios, P.; Gullard, R.; Kadish, K. M. *J. Am. Chem. Soc.* **1984**, *106*, 4472.
- (16) Balch, A. L.; Chan, Y. W.; La Mar, G. N.; Latos-Grazynski, L.; Renner, M. W. *Inorg. Chem.* **1985**, *24*, 1437.
- (17) Balch, A. L.; La Mar, G. N.; Latos-Grazynski, L.; Renner, M. W. *Inorg. Chem.* **1985**, *24*, 2432.

- (18) Wolberg, A.; Monassen, J. *J. Am. Chem. Soc.* **1970**, *92*, 2982.
- (19) Felton, R. H.; Owen, G. S.; Dolphin, D.; Fajer, J. *J. Am. Chem. Soc.* **1971**, *93*, 6332.
- (20) Felton, R. H.; Owen, G. S.; Dolphin, D.; Forman, A.; Borg, D. C.; Fajer, J. *Ann. N. Y. Acad. Sci.* **1973**, *206*, 504.
- (21) Gans, P.; Marchon, J.-C.; Reed, C. A.; Regnard, J.-R. *Nouv. J. Chim.* **1981**, *5*, 203.
- (22) Phillippi, M. A.; Shimomura, E. T.; Goff, H. M. *Inorg. Chem.* **1981**, *20*, 1322.
- (23) Phillippi, M. A.; Goff, H. M. *J. Am. Chem. Soc.* **1982**, *104*, 6026.
- (24) Scholz, W. F.; Reed, C. A.; Lee, Y. J.; Scheidt, W. R.; Lang, G. J. *Am. Chem. Soc.* **1982**, *104*, 6791.
- (25) Buisson, G.; Deronzier, A.; Duee, E.; Gans, P.; Marchon, J.-C.; Regnard, J.-R. *J. Am. Chem. Soc.* **1982**, *104*, 6793.
- (26) Goff, H. M.; Phillippi, M. A. *J. Am. Chem. Soc.* **1983**, *105*, 7567.
- (27) Chin, D. H.; Balch, A. L.; La Mar, G. N. *J. Am. Chem. Soc.* **1980**, *102*, 1446.
- (28) Groves, J. T.; Haushalter, R. C.; Nakamura, M.; Nemo, T. E.; Evans, B. J. *J. Am. Chem. Soc.* **1981**, *103*, 2884.
- (29) Simonneaux, G.; Scholz, W. F.; Reed, C. A.; Lang, G. *Biochim. Biophys. Acta* **1982**, *716*, 1.
- (30) La Mar, G. N.; de Ropp, J. S.; Latos-Grazynski, L.; Balch, A. L.; Johnson, R. B.; Smith, K. W.; Parish, D. W.; Cheng, R. J. *J. Am. Chem. Soc.* **1983**, *105*, 782.
- (31) Penner-Hahn, J. E.; McMurry, T. J.; Renner, M. W.; Latos-Grazynski, L.; Eble, K. S.; Davis, I. M.; Balch, A. L.; Groves, J. T.; Dawson, J. H.; Hodgson, K. O. *J. Biol. Chem.* **1983**, *258*, 12761.
- (32) Balch, A. L.; Chan, Y.-W.; Cheng, R. J.; La Mar, G. N.; Latos-Grazynski, L.; Renner, M. W. *J. Am. Chem. Soc.* **1984**, *106*, 7779.
- (33) Balch, A. L.; La Mar, G. N.; Latos-Grazynski, L.; Renner, M. W.; Thanabal, V. *J. Am. Chem. Soc.* **1985**, *107*, 3003.
- (34) Balch, A. L.; Latos-Grazynski, L.; Renner, M. W. *J. Am. Chem. Soc.* **1985**, *107*, 2983.
- (35) Schappacher, M.; Weiss, R.; Montiel-Montoya, R.; Trautwein, A.; Taburd, A. *J. Am. Chem. Soc.* **1985**, *107*, 3736.
- (36) Loew, G. H.; Herman, Z. S. *J. Am. Chem. Soc.* **1980**, *102*, 6175.
- (37) Hanson, L. K.; Chang, C. K.; Davis, M. S.; Fajer, J. *J. Am. Chem. Soc.* **1981**, *103*, 663.

Scheme I

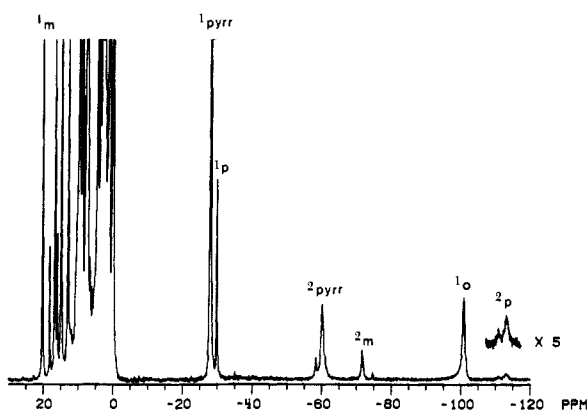
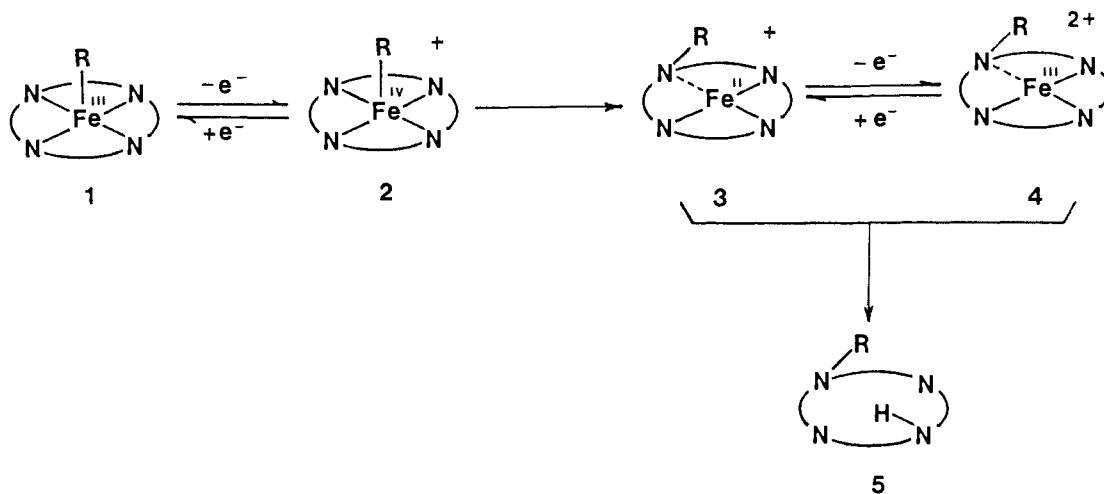
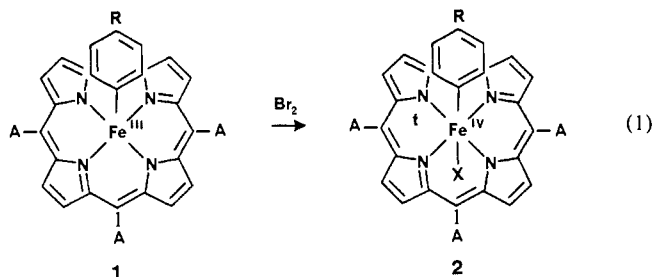


Figure 1. ^1H NMR (360 MHz) spectrum of a sample of **1** ($\text{R} = \text{H}$ and $\text{A} = p\text{-C}_6\text{H}_4\text{CH}_3$) in chloroform-*d* at -50°C after the addition of 0.1 mol of bromine. Resonances of **1** and **2** are identified as such followed by assignments of individual proton resonances: pyrr, pyrrole protons, o, ortho-phenyl iron; m, meta-phenyl iron; p, para-phenyl iron.

Results

The one-electron oxidation of **1** was accomplished by using bromine as the oxidizing agent. In a typical reaction, a chloroform solution of **1** was prepared under dioxygen-free conditions and cooled to -60°C . Bromine in chloroform was added to effect the oxidation. When a substoichiometric amount of bromine was added, separate resonances were observed for **1** and **2** (eq 1) as shown in Figure 1. The appearance of separate resonances for



1 and **2** indicates that the rate of electron transfer is slow. The rate constraint for exchange is estimated to be less than $5 \times 10^{-4} \text{ s}^{-1}$. Addition of more bromine simply converts more **1** to **2**, and a slight excess of bromine has no effect on the spectrum. Other oxidizing agents (I_2 , $(\text{TMP}\cdot)\text{Fe}^{\text{III}}(\text{ClO}_4)_2$), which have been successfully used in other one-electron iron porphyrin oxidations,³⁴ were not capable of oxidizing **1** to **2**.

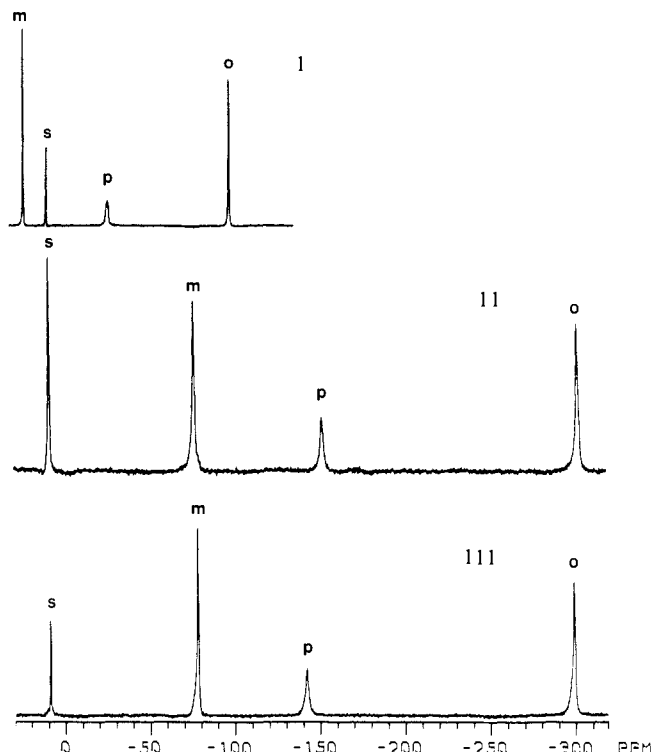


Figure 2. ^2H NMR (77 MHz) spectra of chloroform-*d* solutions at -60°C of (I) **1** ($\text{R} = \text{D}$ and $\text{A} = \text{C}_6\text{H}_5$); (II) **2** ($\text{X} = \text{ClO}_4$) formed by the addition of a slight excess of bromine followed by the addition of silver perchlorate to the sample used for trace I; and (III) **2** ($\text{X} = \text{SbF}_6$) formed by the addition of bromine and AgSbF_6 to **1** ($\text{R} = \text{D}$ and $\text{A} = \text{C}_6\text{H}_5$). The iron-bound phenyl group is deuterium labeled in all positions.

In Figure 1, the resonance assignments for the iron(III) complex **1** follow those previously made.⁵ Additionally, the identity of the pyrrole resonance was confirmed by its absence in the spectrum obtained from pyrrole-deuterated **1**. The resonance assignments for the iron(IV) complex **2** have been determined by relative areas, line widths, specific deuteration, and methyl substitution. The iron-phenyl resonances were most readily identified through the ^2H NMR spectra of iron-phenyl-deuterated **1** and its oxidation products. The spectra are shown in Figure 2. Trace I shows the spectrum of the iron(III) complex **1**, while trace II shows the effect of bromine oxidation followed by the addition of silver perchlorate. Three phenyl resonances are readily observed, and the para proton can be assigned based on its area. The ^2H NMR spectra are particularly valuable in detecting the very high field resonance of **2** at -300 ppm. In the corresponding ^1H NMR spectra, the analogue of this feature is broad, and that, coupled with its unusually large shift, has made it difficult to detect until we knew

(38) Groves, J. T.; Quinn, R.; McMurry, T. J.; Nakamura, M.; Lang, G.; Boso, B. *J. Am. Chem. Soc.* **1985**, *107*, 354.

Table I. ^1H NMR Data for Iron(IV) Complexes in Chloroform- d Solution

compound	chemical shifts, ppm										temp. °C
	Fe-phenyl				porphyrin phenyl					para	
	ortho	meta	para	pyrr	ortho	ortho'	meta	meta'			
$\text{C}_6\text{H}_5\text{Fe}^{\text{IV}}(\text{T-}p\text{-TP})\text{Br}$	<i>e</i>	-71	-113	-60	10.3	9.8	9.5	9.5	4.3 ^d	-50	
$p\text{-CH}_3\text{C}_6\text{H}_4\text{Fe}^{\text{IV}}(\text{TPP})\text{Br}$	-290	-67	114 ^d	-63	11.3	10.9	9.3	9.3	8.4	-60	
$m\text{-CH}_3\text{C}_6\text{H}_4\text{Fe}^{\text{IV}}(\text{TPP})\text{Br}$	<i>e</i>	-89 (-40) ^d	-122	-65	11.4	11.4	8.9	8.9		-60	
$p\text{-CH}_3\text{C}_6\text{H}_4\text{Fe}^{\text{IV}}(\text{TPP})\text{ClO}_4$	<i>e</i>	-66	157 ^d	-71	13.4	12.4	8.1	7.8	9.5	-60	
$m\text{-CH}_3\text{C}_6\text{H}_4\text{Fe}^{\text{IV}}(\text{TPP})\text{ClO}_4$	-311, -320	-89 (-47) ^d	-156	-72	13.4	12.5	8.1	7.8	9.5	-60	
$p\text{-CH}_3\text{C}_6\text{H}_4\text{Fe}^{\text{IV}}(\text{TPP})\text{SbF}_6$	<i>e</i>	-72	114 ^d	-68	15.0	13.8	6.8	6.5	10.4	-60	
$[p\text{-CH}_3\text{C}_6\text{H}_4\text{Fe}^{\text{IV}}(\text{TPP})\text{py}]\text{ClO}_4$	<i>e</i>	-61	156 ^d	-69	11.3	10.0	9.5	9.2	8.2	-60	
$\text{C}_6\text{H}_5\text{Fe}^{\text{IV}}(\text{TMP})\text{Br}^a$	<i>e</i>	-56	-97	-51	4.2 ^d	3.8 ^d	10.6	10.7	3.2 ^d	-50	
$\text{C}_6\text{H}_5\text{Fe}^{\text{IV}}(\text{TMP})\text{ClO}_4^a$	<i>e</i>	-76	-126	-68	3.3 ^d	2.8 ^d	8.3	8.0	3.1 ^d	-50	
$(\text{CH}_3\text{O})_2\text{Fe}^{\text{IV}}(\text{TMP})^b$				-38		2.4 ^d	7.7	7.7	2.9 ^d	-78	
$(\text{CN})_2\text{Mn}^{\text{III}}(\text{TPP})^-^c$				-15		5.7	5.7	5.7	4.3	26	
$(\text{Im})_2\text{Mn}^{\text{III}}(\text{TPP})^-^c$				-18		8.6	8.6	8.6	11.1	26	
$\text{Fe}^{\text{III}}(\text{TPP})\cdot(\text{ClO}_4)_2^f$				-22.6		27.1	-27	-27	20.6	25	
$(\text{Im})_2\text{Fe}^{\text{III}}(\text{TPP})^{2+g}$				-40.1		-31.7	36.4	36.4	-22.1	-38	

^a In toluene- d_8 . ^b In dichloromethane- d_2 /methanol- d_4 from ref 38. ^c In dimethyl- d_6 sulfoxide from ref 42. ^d Methyl resonance. ^e Not observed in ^1H spectrum due to width and large hyperfine shift. ^f In CD_2Cl_2 from ref 25. ^g In CD_2Cl_2 from ref 26.

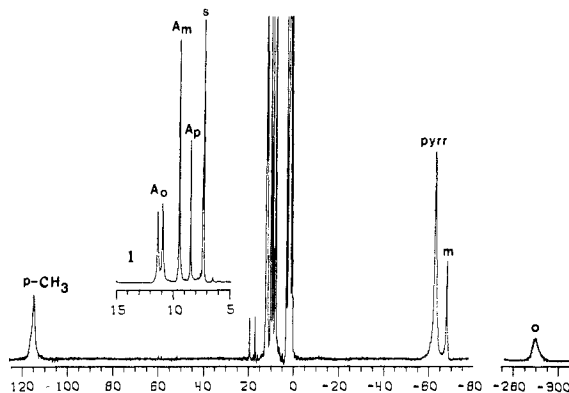


Figure 3. ^1H NMR (360 MHz) spectrum of **2** ($\text{R} = \text{CH}_3$, $\text{X} = \text{Br}$, and $\text{A} = p\text{-C}_6\text{H}_4\text{CH}_3$) in chloroform- d solution at -60°C . Insert I shows an expansion of the 15–5 ppm region. Resonances are labeled as in Figure 1 with A indicating porphyrin aryl protons.

where to look for it. For example, the corresponding feature was not observed in the spectrum used to prepare Figure 1.

Figure 3, which shows the spectrum of a relatively pure sample of **2** ($\text{R} = \text{CH}_3$, $\text{X} = \text{Br}$, and $\text{A} = \text{C}_6\text{H}_5$), allows several other features of the spectrum to be assigned. The appearance of a new resonance at 114 ppm and the absence of a resonance at -118 ppm allows the para-methyl resonance to be assigned and confirms the assignment of the para-phenyl proton in Figures 1 and 2. The resonances in the 5–15 ppm region are assigned to the porphyrin phenyl resonances. They remain at full intensity when the spectrum of pyrrole-deuterated **2** ($\text{R} = \text{H}$, $\text{X} = \text{Br}$, and $\text{A} = \text{C}_6\text{H}_5$) is examined, while the intensity of the resonance at -60 ppm decreases. The resonance at 8.5 ppm is assigned as the porphyrin para-phenyl resonance on the basis of its area and its absence in the spectrum of **2** ($\text{R} = \text{H}$, $\text{X} = \text{Br}$, and $\text{A} = p\text{-C}_6\text{H}_4\text{CH}_3$). The porphyrin ortho- and meta-phenyl resonances were assigned on the basis of their line widths. The relaxation mechanism for porphyrin phenyl protons is predominantly dipolar. Therefore, the ortho protons, which are closer to the iron, will produce broader resonances than the meta protons. Consequently, the two broader resonances at 11 and 11.5 ppm are assigned to the ortho protons. The observation of split ortho resonances is consistent with the lack of symmetry about the porphyrin plane. In contrast, the meta protons, which are further removed from the unsymmetrical axial substituents, are not resolved into the expected two peaks.

The spectral data for a number of substituted forms of **2** are compiled in Table I. The data for the *m*-tolyl iron(IV) complexes on lines 3 and 5 of Table I allow the ortho and meta protons of the iron-bound aryl group to be assigned.

A Curie plot of the temperature dependence of the chemical shifts of the porphyrin and axial phenyl resonances is shown in Figure 4. The resonances show linear behavior with extrapolated

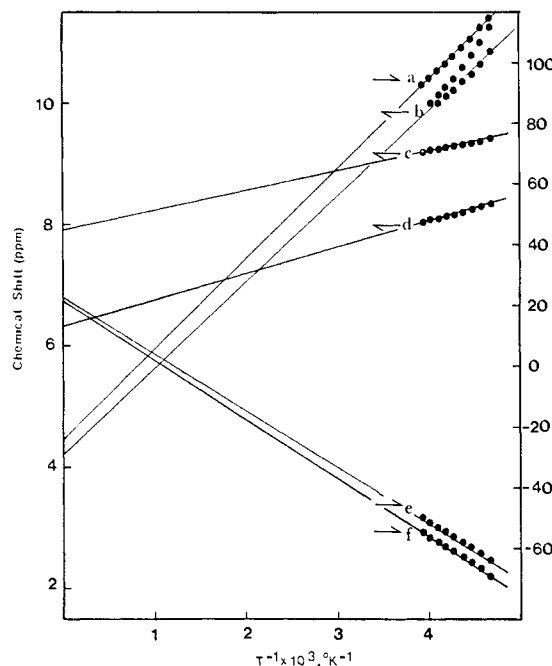


Figure 4. Curie plot for **2** ($\text{R} = \text{CH}_3$, $\text{X} = \text{Br}$, and $\text{A} = \text{C}_6\text{H}_5$) in chloroform- d . Resonances are identified as (a) para-methyl of iron-tolyl, (b) ortho-H of A, (c) meta-H of A, (d) para-H of A, (e) pyrrole-H, and (f) meta-H of iron-tolyl.

intercepts that do not correspond to those of the diamagnetic reference, $\text{C}_6\text{H}_5\text{InTPP}$ (TPP is the dianion of tetraphenylporphyrin).³⁹ The linear Curie plot indicates that only one iron spin state is involved over the accessible temperature range.

The magnetic moment of **2** ($\text{R} = \text{CH}_3$, $\text{X} = \text{Br}$, and $\text{A} = \text{C}_6\text{H}_5$) has been determined by the Evans' technique. At -60°C , the magnetic moment is $2.6 \pm 0.4 \mu_B$. This value is consistent with the presence of a triplet ground state (spin only moment, $2.84 \mu_B$) for **2**.

Axial Ligation. The NMR data indicate that a sixth ligand occupies the site opposite the phenyl group in **2**. Comparison of traces II and III of Figure 2 offers representative data. Trace II shows the spectrum for the perchlorate complex. Trace III shows the effect of adding silver hexafluoroantimonate after bromine oxidation. As can be seen, the spectral pattern is retained, but there are significant changes in the chemical shifts, particularly for the para protons. We ascribe these changes to changes in the axial ligand, and we believe that both of these weakly nucleophilic anions are coordinated. Some further comparative data are given

(39) Cocolos, P.; Guillard, R.; Fournari, P. *J. Organomet. Chem.* 1979, 179, 311.

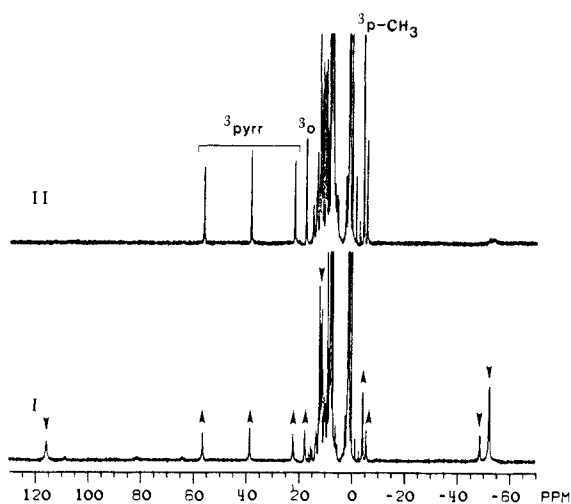
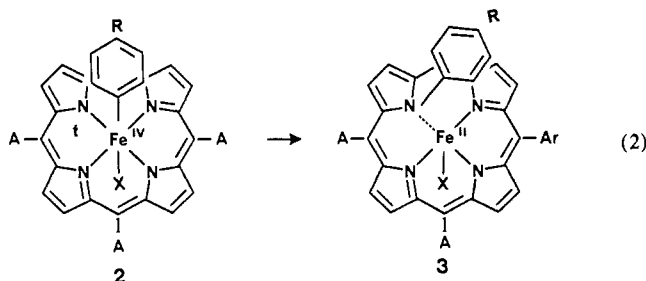


Figure 5. (I) ^1H NMR (360 MHz) spectra of chloroform- d solutions of **2** ($R = \text{CH}_3$, $X = \text{ClO}_4^-$, and $A = \text{C}_6\text{H}_5$) at 0°C . (II) The same after 30 min. Peaks of **2** and **3** are labeled according to the scheme used in Figure 1.

in Table I. Note that with only bromide present, the pattern remains but again the chemical shifts differ.

Further evidence for transaxial ligation comes from studies with pyridine (py). Addition of excess pyridine to **2** ($R = \text{CH}_3$, $X = \text{ClO}_4^-$, and $A = \text{C}_6\text{H}_5$) in chloroform- d at -60°C produces a new ^1H NMR spectrum. The basic pattern of porphyrin and iron- p -tolyl resonances remains, but three additional resonances due to the coordinated pyridine appear at 19 ppm (line width: 120 Hz), -9 ppm (180 Hz) and -17 ppm (770 Hz). The relative peak areas indicate that the peaks at 19 and -17 ppm correspond to two protons, while the peak at -9 ppm corresponds to a single proton. Consequently, the peak at -9 ppm is assigned to the para-pyridine proton. On the basis of line width, the peak at -17 is assigned to the ortho-pyridine protons and the peak at 19 ppm to the meta-pyridine protons. The observation of these resonances establishes axial coordination by one pyridine molecule and indicates that free and bound pyridine are in slow exchange at -60°C .

Phenyl Migration. Upon warming, samples of **2** are unstable. Figure 5 shows the changes which occur on warming a solution of **2** ($R = \text{CH}_3$, $X = \text{ClO}_4^-$, and $A = \text{C}_6\text{H}_5$) to 0°C and allowing it to stand. Trace I shows the spectrum after warming, while trace II shows the same sample after standing at 0°C for 30 min. In trace I, the resonances of **2** are still detectable, while in trace B they have nearly completely gone. In their place, a new set of resonances has appeared. The pattern of these new resonances indicates that they result from **3** ($R = \text{CH}_3$, $X = \text{ClO}_4^-$, and $A = \text{C}_6\text{H}_5$), the iron(II) N - p -tolylporphyrin complex which has formed via eq 2. The ^1H NMR spectra of iron(II) complexes



of N -substituted porphyrins have been previously examined and analyzed in detail.¹⁶ They are characterized by the presence of four pyrrole resonances that result from the lower symmetry of the N -substituted porphyrin. In the case of **3**, three of these are clearly detected in the anticipated downfield region. Their assignment as pyrrole protons has been confirmed by observations on the corresponding pyrrole-deuterated sample, which shows diminished intensity for these three resonances. From previous

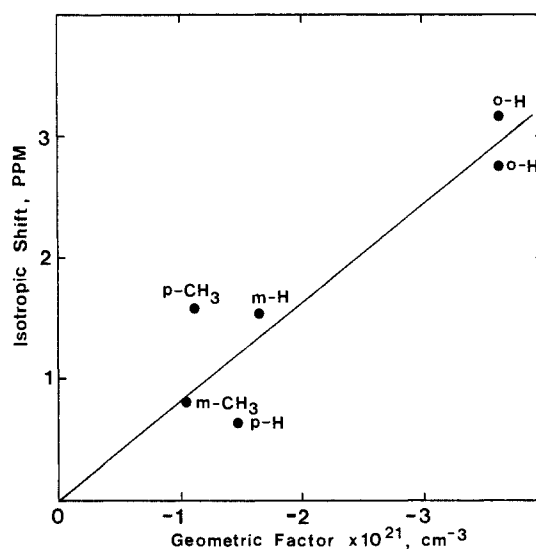


Figure 6. Plot of the isotropic shifts for **2** ($X = \text{Br}$) at -60°C in chloroform- d solutions vs. the calculated geometric factor $(3 \cos^2 \theta - 1)r^{-3}$. Only resonances of porphyrin aryl groups (A) are plotted.

work, it is anticipated that the fourth pyrrole resonance will lie in the 10 to -5 ppm region. In Figure 5, this region is congested with other resonances so that identification of the fourth pyrrole resonance cannot be made. Two other tentative assignments of resonances in trace B can be made. The peak at 20 ppm is assigned as an porphyrin ortho-phenyl resonance on the basis of its intensity, the presence of a similar downfield-shifted ortho-phenyl resonance in other N -substituted iron(II) complexes,¹⁶ and its absence in the corresponding spectrum of the complex derived from tetramesitylporphyrin. On the basis of its intensity and comparison with the spectrum obtained on warming **2** ($R = \text{H}$, $X = \text{ClO}_4^-$, and $A = \text{C}_6\text{H}_5$), the resonance at -4 ppm is assigned to the para-methyl protons of the iron-bound tolyl group.

The transformation of **2** to **3** is accompanied by a marked color change from deep red to green. The optical spectrum of the sample after warming shows a pattern (λ_{max} 440, 460 sh, Soret, 574, 610, 656 nm) which is characteristic of a divalent metal- N -substituted porphyrin complex.

Discussion

Analysis of the Electronic Structure of the Iron(IV) Complexes.

The hyperfine shifts, the differences between the observed shifts for paramagnetic complex, and the corresponding shifts of an analogous diamagnetic complex (in this case the In(III) analogue of **1**)³⁹ observed in the NMR spectra are the sum of the scalar or contact contribution, which reflects the mode of spin delocalization, and the dipolar shift, which is due to the magnetic anisotropy of the iron. In the limit of axial symmetry, the dipolar shift is given by eq 3 where N is Avogadro's number, χ_{\parallel} are χ_{\perp}

$$\frac{\Delta H_{\text{dip}}}{H} = \frac{1}{3N} (\chi_{\parallel} - \chi_{\perp}) \frac{3 \cos^2 \theta - 1}{r^3} \quad (3)$$

are the magnetic susceptibilities parallel and perpendicular to the z axis (taken as coincident with the iron-phenyl bond), and r and θ are the usual polar coordinates.⁴⁰ Separation of the dipolar and contact terms can be made by examining a plot of the isotropic shift vs. the geometric factor, $(3 \cos^2 \theta - 1)r^{-3}$. This graph should yield a linear plot so long as the porphyrin aryl protons on **2** are effectively isolated (by virtue of their nearly perpendicular orientation to the porphyrin plane) from contact spin density within the iron/porphyrin core.⁴¹ Such a plot for the bromoiron(IV) complex **2**, using the geometrical data available on **1** ($R = \text{H}$ and

(40) Horrocks, W. D. In "NMR of Paramagnetic Molecules"; La Mar, G. N., Horrocks, W. D., Holm, R. H., Eds.; Academic Press: New York, 1973; pp 127-177.

(41) La Mar, G. N.; Walker (Jensen), F. A. In "The Porphyrins"; Dolphin, D., Ed.; Academic Press: New York, 1979; Vol. 4, p 61.

Table II. Separation of Dipolar and Contact Shifts for Iron(IV) Complex **2** (X = Br)

position	$\Delta H/H_{iso}$	$\Delta H/H_{dip}$	$\Delta H/H_{con}$	GF, ^{a,b} 10 ²¹ cm ⁻³	rel ^{a,b} GF
Porphyrin Phenyl					
<i>o</i> -H	3.16	2.76	0.4	-36.0 ^a	1
<i>o</i> -H	2.76	2.76	0	-36.0 ^a	
<i>m</i> -H	1.54	1.28	0.26	-16.7 ^a	0.46
<i>p</i> -H	0.4	1.13	-0.49	-14.8 ^a	0.41
<i>m</i> -CH ₃	0.8	0.805	-0.005	-10.5 ^a	0.29
<i>p</i> -CH ₃	1.58	0.84	0.74	-11.0 ^a	0.31
pyrr	-72.0	5.39	-77.4 ^c	-70.3 ^a	1.95
Iron Phenyl					
<i>o</i> -H	-293	-16.6	-276	217	-6.0
<i>m</i> -H	-73	-8.8	-64	115	-3.2
<i>p</i> -H	-119	-8.0	-111	106	-2.9
<i>m</i> -CH ₃	-43	-4.8	-38.2	63	-1.75
<i>p</i> -CH ₃	112	-5.0	+117	66	-1.8

^aGeometric factor $(3 \cos^2 \theta - 1)r^{-3}$. ^bTaken from: La Mar, G. N.; Bold, T. J.; Satterlee, J. D. *Biochim. Biophys. Acta* **1977**, *498*, 189. ^cThe corresponding shifts (at 25 °C) for (Im)₂Mn^{III}(TPP)⁻ and (NC)₂Mn^{III}(TPP)⁻ are -33.6 and -16.8, respectively.

A = C₆H₅),⁶ is shown in Figure 6. The linearity of this plot indicates effective isolation of the porphyrin aryl groups from unpaired spin delocalization and allows the separation of the contact and dipolar contributions. The results of this analysis are given in Table II.

The contact contribution to the porphyrin portion of the spectrum can be used to discriminate between the two likely electronic structures: a low-spin iron(IV) coordinated by a conventional porphyrin dianion or a iron(III) bound to a oxidized porphyrin radical monoanion. The d orbital occupancy for an iron(IV) ion in *D*_{4h} symmetry is *d*_{xy}², *d*_{xz}¹, *d*_{yz}¹, *d*_{z²}⁰, *d*_{x²-y²}⁰, and therefore, unpaired spin is in orbitals of π symmetry. Similar occupancies occur in the isoelectronic, low-spin manganese(III) complexes (TPP)Mn(CN)₂⁻ and (TPP)Mn(Im)₂⁻ (Im is imidazole),⁴² and (TMP)Fe(OCH₃)₂.³⁸ There are striking similarities between the NMR spectra of **2** and these manganese(III) and iron(IV) complexes. As shown in Table II, the pyrrole contact shifts in **2** and in the manganese(III) complexes are similar and indicative of π -spin delocalization. Moreover, the porphyrin aryl protons in **2** and in the manganese(III) complexes show primarily dipolar shifts and insulation from π -spin contact shifts.⁴² Likewise (TMF)Fe(OCH₃)₂ displays upfield-shifted pyrrole resonances in the general vicinity of those in **2** as well as small hyperfine shifts for the mesityl protons.³⁸

In contrast, complexes containing oxidized porphyrin radicals display very different spectral patterns. The complexes, Fe^{III}(·P)(ImH)₂⁺ (·P is a porphyrin radical monoanion), obtained by addition of ImH to Fe^{III}(·P)Cl(ClO₄)₂,²⁶ are of particular relevance since they have a magnetic susceptibility ($2.8 \pm 0.2 \mu_B$) similar to that observed for **2**. The pyrrole resonances for Fe^{III}(·P)(ImH)₂⁺ fall in a range -30 to -40 ppm (at -38 °C) that is similar to **2**. However, the porphyrin aryl protons of Fe^{III}(·P)(ImH)₂⁺ show sizeable hyperfine shifts: for Fe^{III}(·TPP)(ImH)₂⁺, the chemical shifts at -38 °C are ortho protons, -31.7 ppm; meta protons, 30.4 ppm; and para protons, -22.1 ppm. Other complexes believed to contain porphyrin radicals also show large hyperfine shifts for the porphyrin phenyl resonances.^{22,25,26,34} This is the most distinctive difference between **2** and the complexes containing porphyrin radicals. In fact, the behavior of the aryl protons shown in Figure 6 is the antithesis of what is found for iron complexes containing an oxidized porphyrin radical.

This conclusion is entirely in accord with the information available from electronic spectra. Lancon et al.¹⁵ previously concluded from the transient electronic spectrum obtained after electrochemical oxidation of C₆H₅Fe(OEP) (OEP = octaethylporphyrin dianion) that iron rather than porphyrin oxidation had occurred. They were unable to detect the TPP analogue due to

its short lifetime, but our electronic spectral data are in substantial agreement with the data on the OEP system. In particular, chemically generated **2** is red with a Soret band at 416 nm and lacks low-energy absorption that is characterized of porphyrin radicals.^{19,20}

The protons of the iron-bound phenyl group display substantial hyperfine shifts. Indeed the presence of three, far upfield phenyl resonances should serve as an excellent diagnostic probe for detecting **2**, particularly in a protein environment. The observation of contact shifts of comparable magnitude and opposite sign for the para proton and para-methyl group on **2** along with the fact that the shifts for the iron-phenyl protons do not attenuate in the order ortho > meta > para as one moves away from the iron suggests that the unpaired spin resides in a π orbital of the phenyl ring. This is, of course, what is expected since the unpaired spins on the iron reside in π -type orbitals. However, the behavior of the meta resonances is not indicative of pure π -spin delocalization. Thus, the meta contact shift has the same sign as the ortho and para shifts, and there is no reversal in its sign upon methyl substitution. Consequently, there must be some degree of π unpaired spin delocalization which probably results from a polarization mechanism, a feature frequently encountered in pyridine which is isoelectronic with the phenyl ligand.⁴³

It is instructive to compare the NMR spectra of **1** and **2**. Except for the iron-*m*-phenyl resonances, there is considerable similarity in the overall spectral pattern. The other major differences are the greater hyperfine shifts seen for the iron(IV) complex **2**. This is not at all surprising. The iron(III) complex has the orbital occupancy (*d*_{xy})², (*d*_{xz}, *d*_{yz})³, (*d*_{z²})⁰, (*d*_{x²-y²})⁰ and one less unpaired electron in orbitals of π symmetry. As a direct consequence, the hyperfine shifts for **1**, which are primarily contact in origin,⁴⁴ are all reduced in comparison to those of **2**.

On the other hand, the NMR spectra of **2** and porphyrin complexes containing the (Fe^{IV}O)²⁺ group are entirely different. Six-coordinate (py)(TPP)Fe^{IV}O^{27,30,32} and five-coordinate (TMP)Fe^{IV}O³² display ¹H NMR spectra in which the porphyrin resonances show extremely small hyperfine shifts. These small shifts are entirely consistent with theoretical calculations,^{36,37} which indicate substantial π interaction between iron and oxygen orbitals and effective localization of unpaired spin density within the (Fe^{IV}O)²⁺ unit.

It is clear that the axial ligands play a major role in determining the electronic distribution within highly oxidized iron porphyrins. Thus, an oxo ligand, a phenyl ligand, or two methoxy ligands favor the iron(IV) porphyrin dianion structure, while halide ions, imidazole, or perchlorate ligand produce the iron(III) porphyrin radical monoanion structure. Interaction of the iron π electron with the axial ligand must make a major contribution to these differences.

Phenyl Migration. The NMR spectra of **1** and **2** are indicative of full *D*_{4h} symmetry with a freely rotating, iron-bound phenyl group. The thermally unstable **2** is converted cleanly into **3** upon warming. This process is a classic example of a reductive elimination of two anionic ligands (the phenyl group and a deprotonated pyrrole) which are already in the required cis positions.⁴⁵ A very effective parallel is seen in the reductive coupling of alkyl fragments in dialkylbis(α,α' -bipyridine)iron(II) where oxidation to the iron(IV) state results in selective coupling of the two alkyl groups to form the corresponding alkane, while release of the alkyl groups at the iron(II) level of oxidation proceeds via β -hydride transfer and at the iron(III) level involves radical formation.⁴⁶ Other cases of phenyl migration from cobalt to porphyrin nitrogen are known.⁴⁷⁻⁴⁹

(43) La Mar, G. N. In "NMR of Paramagnetic Molecules"; La Mar, G. N., Horrocks, W. Dew., Jr., Holm, R. H., Eds.; Academic Press: New York, 1973; p 86.

(44) Balch, A. L.; Renner, M. W. *Inorg. Chem.* **1986**, *25*, 303.

(45) Collman, J. P.; Hegedus, L. S. "Principles and Applications of Organotransition Metal Chemistry"; University Science Books: Mill Valley, CA, 1980; p 232.

(46) Lau, W.; Huffman, J. C.; Kochl, J. K. *Organometallics* **1982**, *1*, 155.

(47) Dolphin, D.; Halko, D. J.; Johnson, E. *Inorg. Chem.* **1981**, *20*, 4348.

(48) Callot, H. J.; Metz, F.; Cromer, R. *Nouv. J. Chim.* **1984**, *8*, 759.

(42) Hansen, A. P.; Goff, H. M. *Inorg. Chem.* **1984**, *23* 4519.

The phenyl migration occurs under aerobic conditions in protein systems, and we have made some observations relevant to the involvement of dioxygen in that process. Addition of limited amounts of dioxygen to **1** in chloroform-*d* at $-60\text{ }^\circ\text{C}$ results in the formation of both **2** and **3**. Thus, dioxygen is fully capable of effecting the iron(III) to iron(IV) oxidation required in eq 1.

Experimental Section

Materials. Dioxygen was removed from chloroform-*d* by three freeze-pump-thaw cycles, and the solvent was placed in a Vacuum Atmospheres glovebox under an argon atmosphere and stored over 4-Å molecular sieves. Phenylmagnesium bromide and *p*-tolylmagnesium bromide were purchased from Aldrich Chemical Co. and Alfa. Phenyl-*d*₅-magnesium bromide and *m*-tolylmagnesium bromide were synthesized by using standard procedures. The iron(III)-phenyl complexes were prepared from the appropriate porphyrin and Grignard reagent by using an established procedure.⁵ Pyrrole-deuterated (TPP)H₂ was prepared according to a standard procedure.⁵⁰

Oxidation of 1. A chloroform solution of **1** was prepared under an argon atmosphere, placed into an NMR tube, sealed using a rubber septum cap, and wrapped with parafilm. In a typical experiment, a 3 mM solution of **1** was cooled to $-60\text{ }^\circ\text{C}$ and titrated with a bromine/chloroform solution (via a syringe). The sample was gently shaken and its color changed from light to dark red. The progress of the reaction was followed by NMR spectroscopy.

Magnetic Susceptibility Measurement. The solution magnetic measurements were made at $-60\text{ }^\circ\text{C}$ by using the Evans' method⁵¹ with tetramethylsilane as the reference. The sample purity was confirmed

(49) Callot, H. J.; Cromer, R.; Louati, A.; Gross, M. *Nouv. J. Chim.* **1984**, *8*, 765.

(50) Boersma, A. D.; Goff, H. M. *Inorg. Chem.* **1982**, *21*, 581.

(51) Evans, D. F. *J. Chem. Soc.* **1959**, 2003.

before and after the measurements were made. The iron porphyrin concentration was determined by UV-vis spectroscopy after the sample was warmed to room temperature by converting it to (TPF)FeCl through treatment with gaseous hydrogen chloride. The original sample of **2** (R = CH₃, X = Br, and A = C₆H₅) contained 13% (TPP)FeCl and (TP-P)FeBr as determined from the NMR spectrum. The magnetic susceptibility (after correction for the iron(III) impurity with an assumed susceptibility of 5.9 μ_B) was 2.6 ± 0.4 μ_B for **2**.

Instrumentation. NMR spectra were obtained on Nicolet NT-360 FT and NM-500 spectrometers operating in the quadrature mode (¹H frequencies are 360 and 500 MHz, respectively). Between 200 and 1000 transients were accumulated over a 40-kHz bandwidth with 16K data points for ¹H (4–8K for ²H) and a 6-μs 90° pulse. The signal-to-noise ratio was improved by apodization of the free induction decay which introduced a negligible 3–10-Hz line broadening. The peaks were referenced against tetramethylsilane. Electronic spectra were measured with a Hewlett-Packard 8450 A spectrophotometer.

Acknowledgment. We thank the National Institutes of Health (Grant GM26226) for support and Dr. M. M. Olmstead for some calculations.

Registry No. **1** (R = H; A = *p*-C₆H₄CH₃), 87607-84-9; **1** (R = D; A = C₆H₅), 101248-90-2; **2** (R = H; X = Br; A = C₆H₅), 101248-78-6; **2** (R = *p*-CH₃; X = Br; A = C₆H₅), 101248-79-7; **2** (R = *m*-CH₃; X = Br; A = C₆H₅), 101248-80-0; **2** (R = *p*-CH₃; X = ClO₄; A = C₆H₅), 101248-81-1; **2** (R = *m*-CH₃; X = ClO₄; A = C₆H₅), 101315-90-6; **2** (R = *p*-CH₃; X = SbF₆; A = C₆H₅), 101248-83-3; **2** (R = H; X = Br; A = *p*-CH₃C₆H₄), 101248-86-6; **2** (R = H; X = ClO₄; A = *p*-CH₃C₆H₄), 101248-87-7; **2** (R = D; X = ClO₄; A = C₆H₅), 101248-91-3; **3** (R = *p*-CH₃; X = ClO₄; A = C₆H₅), 101248-92-4; [*p*-CH₃C₆H₄Fe^{IV}(TPP)-Py]ClO₄, 101248-85-5; (CH₃O)₂Fe^{IV}(TMP), 101248-88-8; Fe^{III}-(TPP)(ClO₄)₂, 83435-87-4; (Im)₂Fe^{III}(TPP)²⁺, 101248-89-9; (CN)₂-Mn^{III}(TPP)⁻, 93383-76-7; (Im)₂Mn^{III}(TPP)⁻, 75120-59-1; Br₂, 7726-95-6.

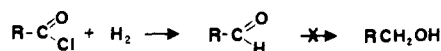
Metamorphosis of Palladium and Its Relation to Selectivity in the Rosenmund Reaction

Wilhelm F. Maier,*† Susan J. Chettle,† Raghav S. Rai,‡ and Gareth Thomas‡

Contribution from the Department of Chemistry and the Department of Materials Science and Mineral Engineering, University of California, Berkeley, California 94720, and the Center for Advanced Materials and the National Center for Electron Microscopy, Materials and Molecular Research Division, Lawrence Berkeley Laboratory, University of California, Berkeley, California 94720. Received June 13, 1985

Abstract: Drastic changes in morphology and particle sizes of the Pd particles were detected during the classical catalyst pretreatment. These changes are connected to the increase in selectivity as well as to the problems encountered in the Rosenmund reaction. A major action of the poison in Rosenmund reactions was found to be the acceleration of the initial reconstruction of the surface of fresh catalysts to prevent overreduction. The instability of the Pd under reaction conditions appears to be responsible for typical problems encountered with the Rosenmund reaction such as irreproducibility and catalyst deactivation during the reaction. With the use of Pd single crystals stepped and kinked surfaces were found to be active for the hydrogenolysis of acid chlorides to aldehydes. Transmission electron microscopy and diffraction have been employed to characterize the change in dispersion and structure of Pd particles on carbon supports after various pretreatments.

The reduction of acid chlorides discovered by Sayzeff in 1872¹ and exploited by Rosenmund,^{1b} was for a long time the only useful method to convert carboxylic acids and derivatives into the corresponding aldehyde. The reaction is based on a supported Pd catalyst and special reaction conditions had been developed to prevent the undesired overreduction.



* Department of Chemistry and the Center for Advanced Materials.

† Department of Materials Science and Mineral Engineering and the National Center for Electron Microscopy.

It has been found that the reduction of the aldehyde formed can be prevented by the use of suitable catalyst "poisons", "modifiers", or "regulators" which deactivate the catalyst selectively. Much attention has been paid to the development of such regulators,² which consist of quinoline with sulfur,³ pyridine and copper,⁴ thiophen or thiourea,⁵ dimethylaniline,⁶ ethyldiiso-

(1) (a) Saytzeff, M. *J. Prakt. Chem.* **1973**, *6*, 130. (b) Rosenmund, K. *W. Chem. Ber.* **1918**, *51*, 585. Rosenmund, K. W.; Zetzsche, F. *Ibid.* **1921**, *54*, 425.

(2) Mosettig, E.; Mazingo, R. *Org. React.* **1948**, *4*, 362.

(3) Weygand, C. M.; Meusel, W. *Chem. Ber.* **1943**, *76*, 498, 503. Hershberg, E. B.; Cason, J. *Org. Synth.* **1941**, *21*, 84.

(4) Ito, T.; Watanabe, K. *Bull. Chem. Soc. Jpn.* **1968**, *41*, 419.